

## Elucidation of Structures and Lithium Environments for an Organo-Sulfur Cathode

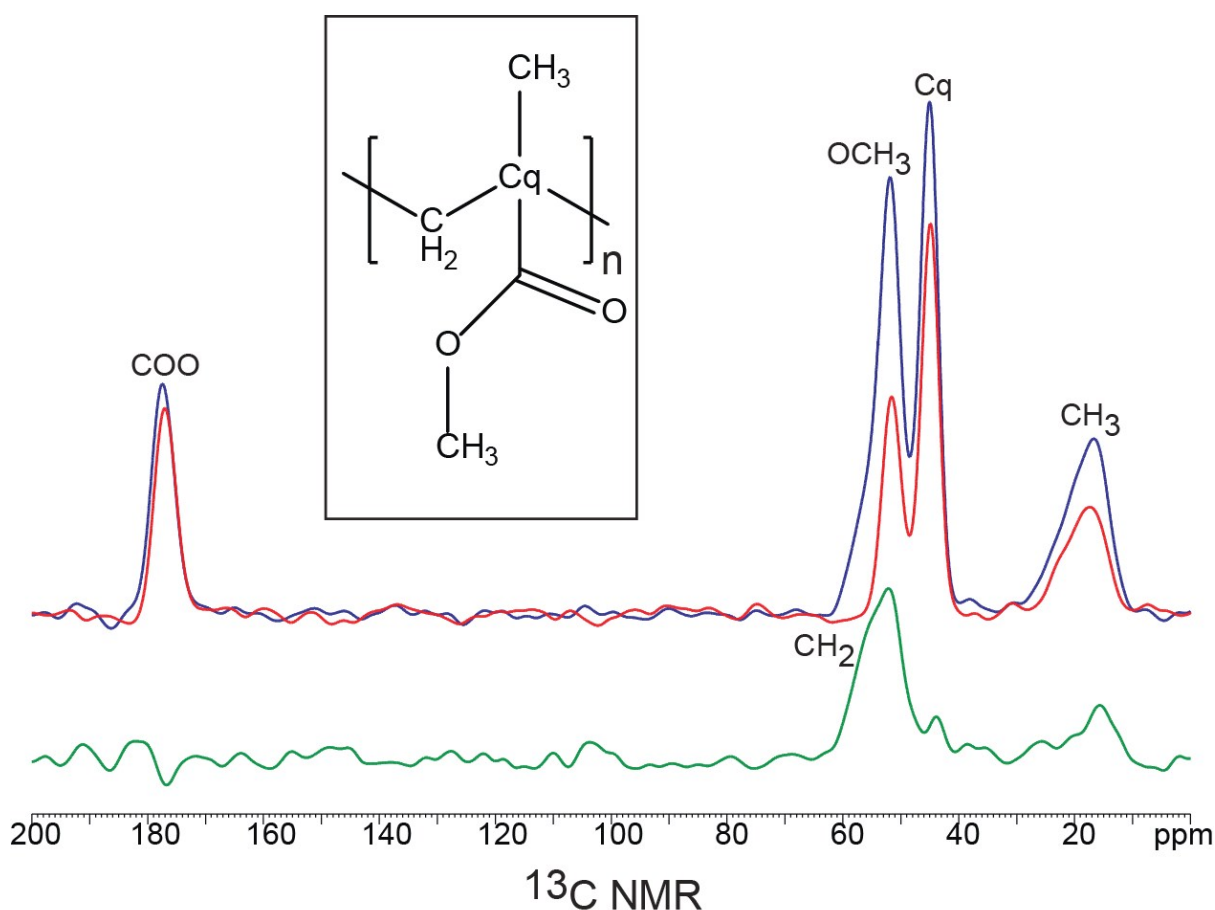
Lisa Djuandhi<sup>1</sup>, Neeraj Sharma<sup>1,\*</sup>, Bruce C. C. Cowie<sup>2</sup>, Thanh V. Nguyen<sup>1</sup>, Aditya Rawal<sup>3</sup>.

<sup>1</sup>School of Chemistry, UNSW Sydney, NSW 2052, Australia

<sup>2</sup>Australian Synchrotron, Clayton, Victoria 3168, Australia

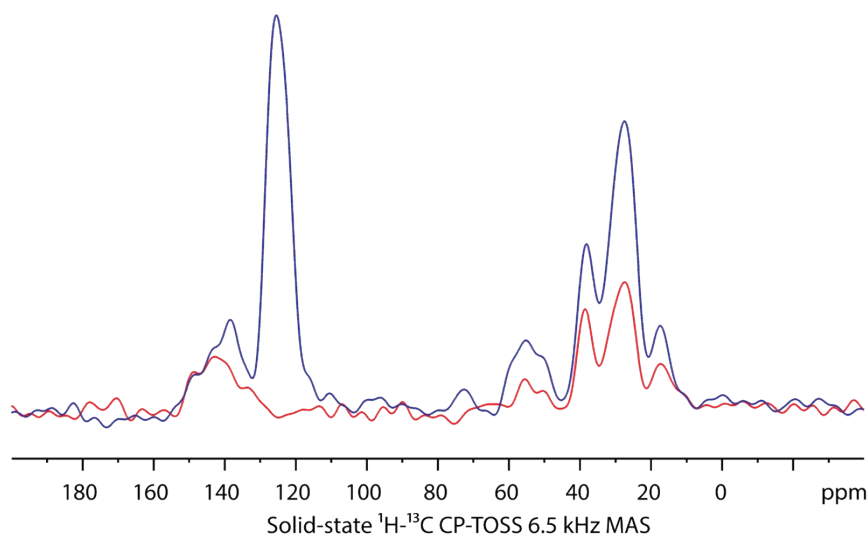
<sup>3</sup>Mark Wainwright Analytical Centre, UNSW Sydney, NSW 2052, Australia

### Supporting Information



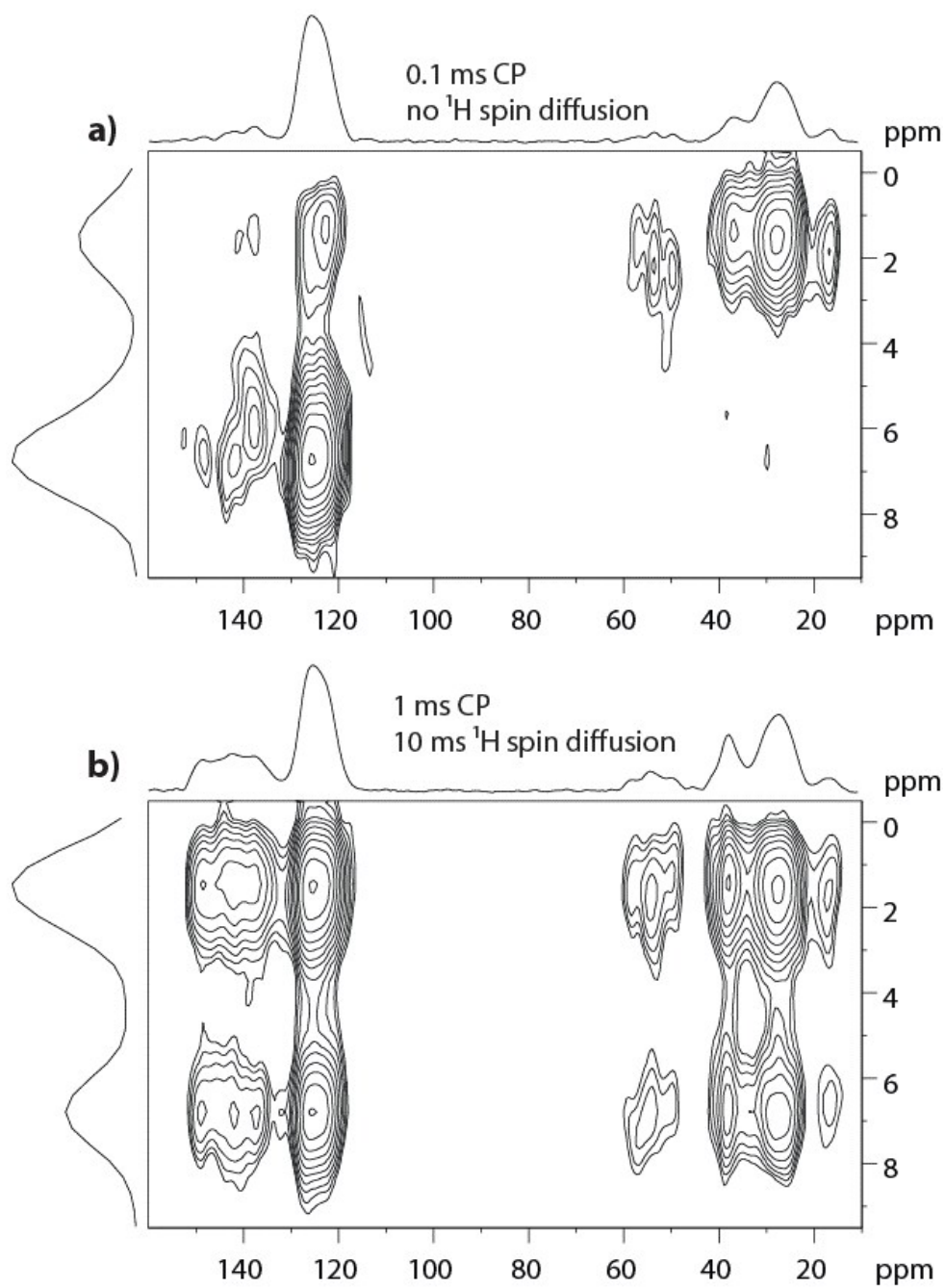
**Figure S1.** <sup>13</sup>C SSNMR spectrum of poly(methyl methacrylate). The spectrum in blue is the <sup>13</sup>C NMR signal of all the carbon species while the spectrum in red is the signal acquired after 40 μs of gated decoupling. Spectrum in green is a scaled difference between the red and blue spectra which identifies the broad signal of the CH<sub>2</sub> species.

Figure S1 demonstrates the effect of the gated decoupling to identify different functional groups in a rigid polymer. The rigid CH<sub>2</sub> species undergo near complete signal suppression, while the rotational mobility of the CH<sub>3</sub> and OCH<sub>3</sub> groups results in partial signal suppression and the nonprotonated carbon species undergo minimal signal suppression.



**Figure S2.** <sup>13</sup>C CP MAS NMR of poly(*S-r*-DIB) acquired after 200 μs of cross-polarization. The spectrum in blue is the <sup>13</sup>C NMR signal of all the carbon species while the spectrum in red is the signal acquired after 40 μs of gated decoupling.

Figure S2 confirms the assignment of the signal at 50-60 ppm range as CH<sub>2</sub> species as opposed to quaternary carbon sites. The use of a relatively short cross polarization time of 200 μs preferentially selects the rigid components of the copolymer, in particular the CH<sub>2</sub> species, which are then effectively suppressed by the the gated decoupling. Note that in comparison to the spectrum in Figure 1 of the main manuscript, which was acquired after a 1 ms cross polarization time, the peaks at 48 ppm and 53 ppm are significantly suppressed. This is strong evidence that the aforementioned peaks correspond to sites with increased motional dynamics, which requires a longer cross polarization time to detect.



**Figure S3.**  $^1\text{H}$ - $^{13}\text{C}$  HETCOR SSNMR spectra of poly(*S-r*-DIB) with **a)** 0.1 ms CP and no  $^1\text{H}$  spin diffusion and **b)** 1 ms CP and 10 ms  $^1\text{H}$  spin diffusion.

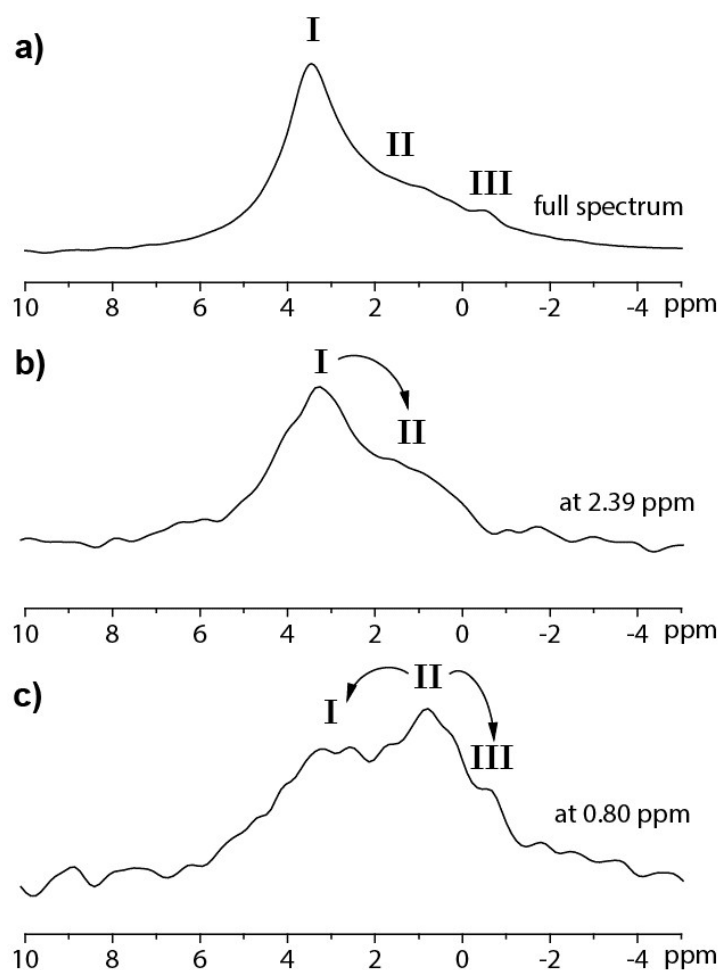


**Figure S4. a)**  $^7\text{Li}$  SSNMR spectrum of the poly(S-*r*-DIB) electrode extracted at the discharged state after 1 cycle (not rinsed with DME solvent), showing 3 distinct lithium environments labelled I, II and III. Slices of the  $^7\text{Li}$ - $^7\text{Li}$  EXSY SSNMR spectrum of the same sample where cross peaks are observed are shown in **b)** wherein a correlation between I-II is observed and **c)** where correlations between I-II and II-III are observed. A correlation between I-III is not observed.

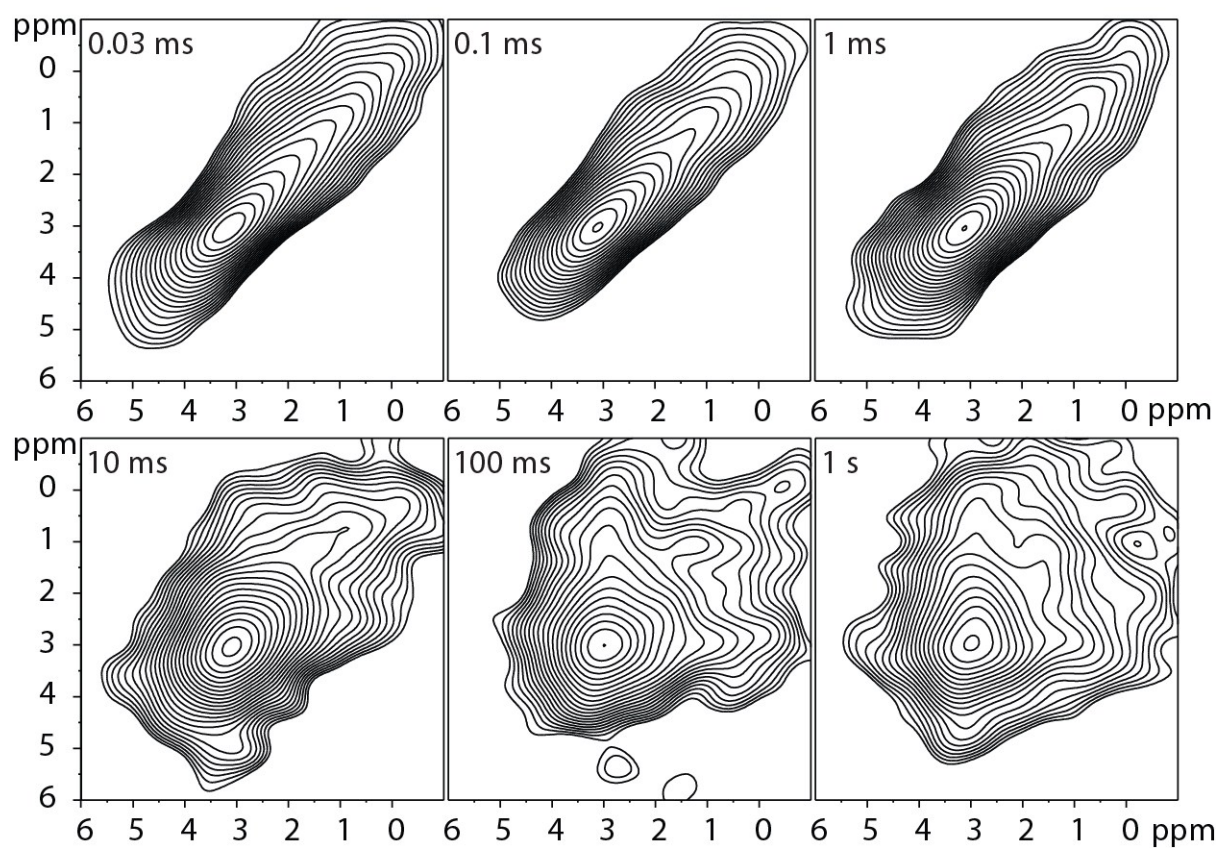


**Figure S5.**  ${}^7\text{Li}$ - ${}^7\text{Li}$  EXSY NMR spectra of the poly(S-*r*-DIB) electrode extracted at the discharged state after one cycle shown at different mixing times  $d_8 = 0.03$  ms, 0.1 ms, 1 ms, 10 ms, 100 ms, and 1 s.

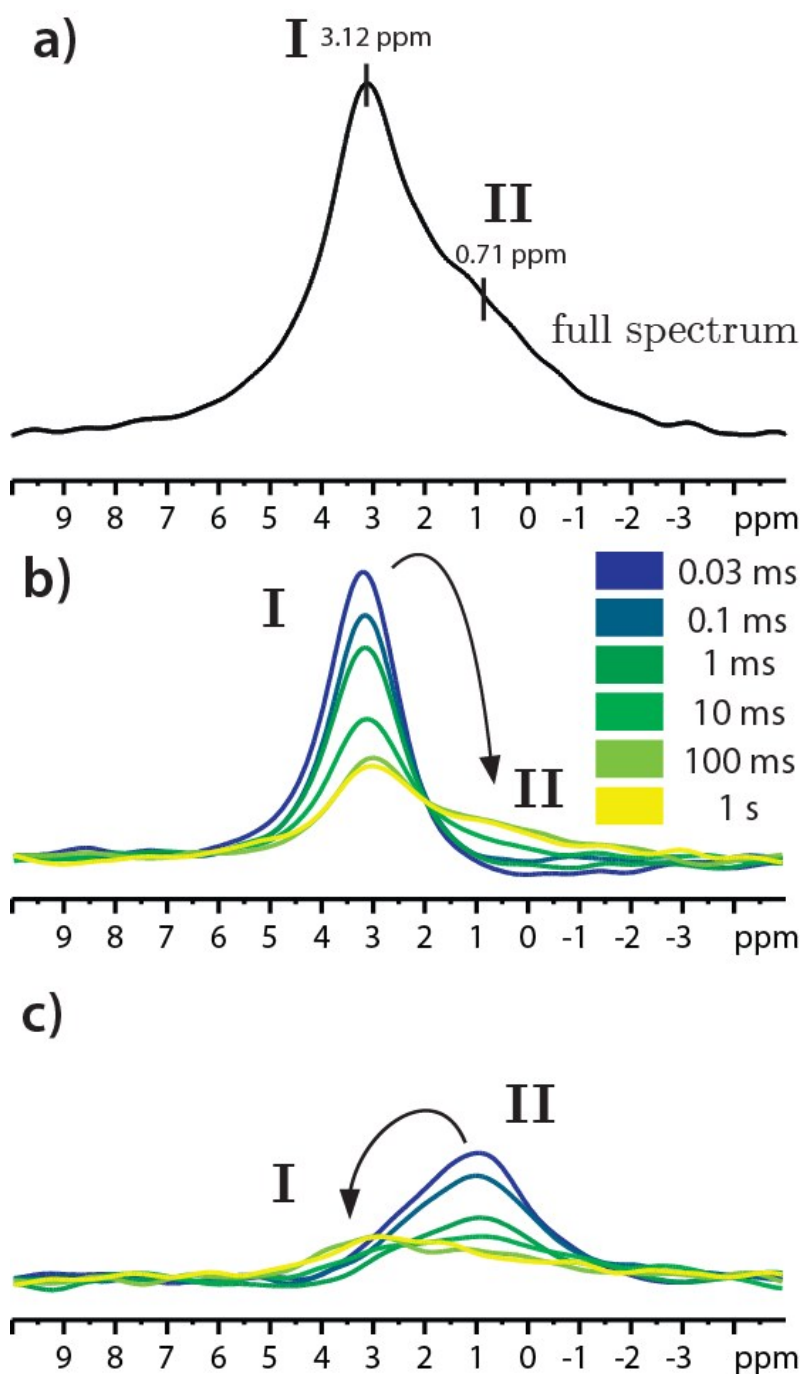


**Figure S6.** **a)** is the full  $^7\text{Li}$  CP/MAS spectrum of the rinsed poly(S-*r*-DIB) cathode after 1 discharge, **b)** are slices from the 2D EXSY in Figure S5 at 3.12 ppm (environment (I)) and **c)** are slices from the 2D EXSY in Figure S5 collected at 0.71 ppm (environment (II)). The line colours indicate the different mixing times. The arrows on **b)** and **c)** indicate the correlation between environments (I) and (II) over longer mixing times.

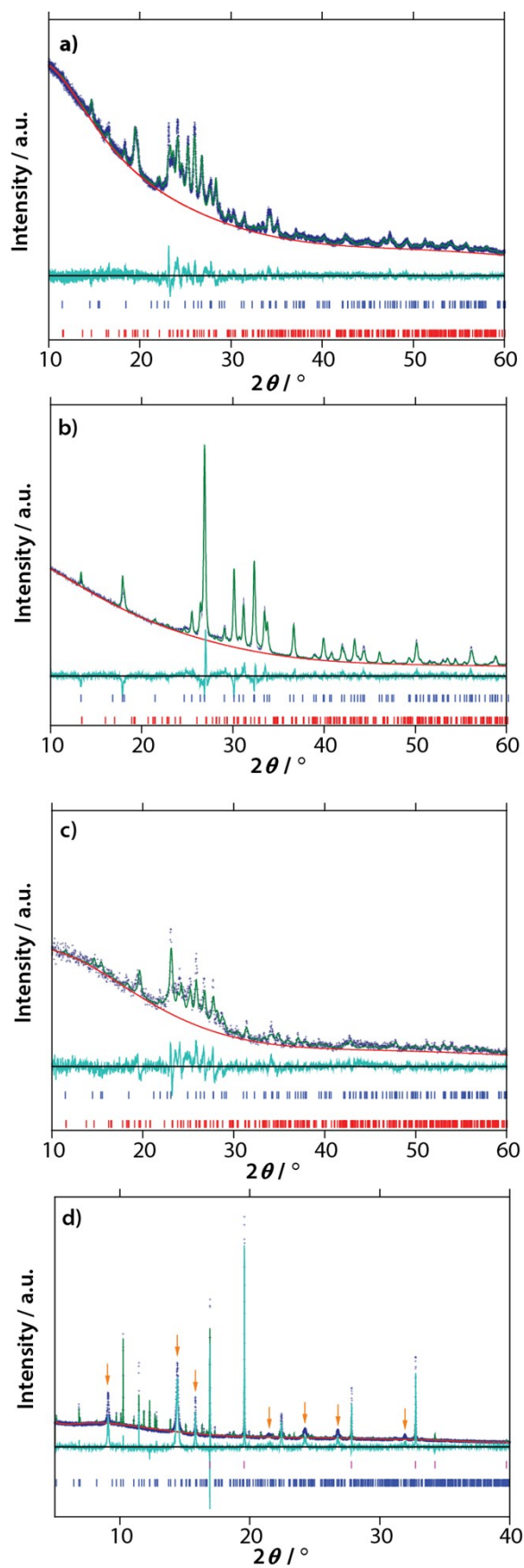


**Figure S7.** Enlarged XRD patterns from Fig. 3. **a)** Rietveld analyses on powder XRD data of as-synthesised poly(*S-r*-DIB) ( $R_p = 2.61\%$ ,  $R_{wp} = 3.69\%$ ), **b)** – the electrode powder used in literature

( $R_p = 3.95\%$ ,  $R_{wp} = 6.03\%$ ), **c**) – a modified electrode powder replacing the polyethylene and chloroform binder with polyvinylidene difluoride (PVDF) and n-methyl pyrrolidone (NMP) ( $R_p = 6.26\%$ ,  $R_{wp} = 8.67\%$ ) and **d**) – in situ synchrotron powder XRD data of this modified electrode examined inside a fresh Li-S cell using 0.38 M lithium bis(trifluoromethane)sulfonimide, 0.31 M lithium nitrate in a 1:1 (v/v) mixture of 1,3-dioxolane and 1,2-dimethoxy ethane as an electrolyte ( $R_p = 12.53\%$ ,  $R_{wp} = 22.74\%$ ). The navy crosses represent the powder XRD data, green line shape the Rietveld fit of models for  $\alpha$ -sulfur (orthorhombic  $S_8$  Fddd:2, ICDD, No. 01-078-1888, blue peak markers) and  $\beta$ -sulfur (monoclinic  $S_8$  P21/c, ICDD No. 01-071-0137, red peak markers). The red line shape represents the calculated background and teal line the residual signal. The orange arrows in **d**) indicate components of the cell that are not accounted for, and the lilac peak markers indicate aluminium that is found in the cell casing.

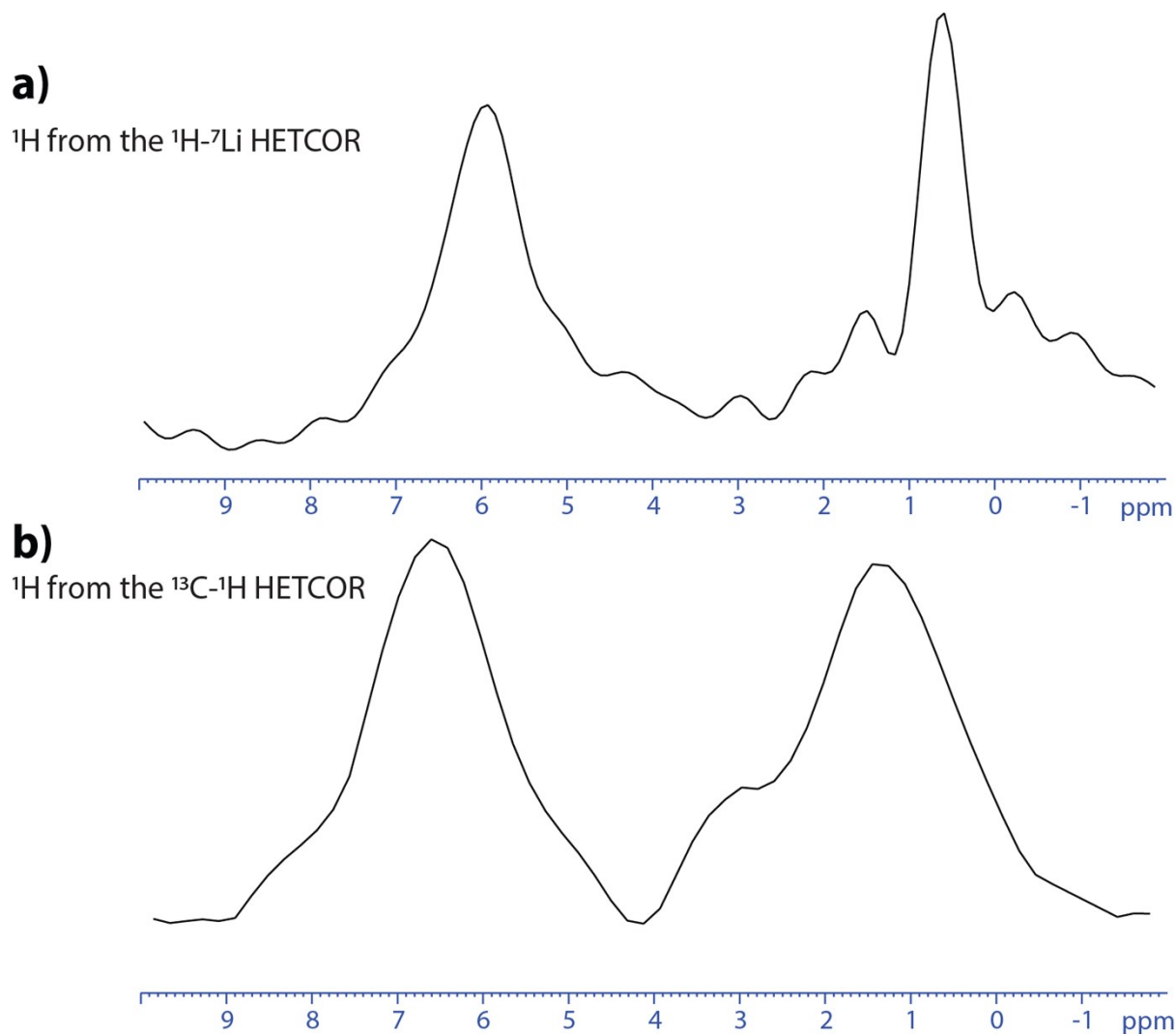


**Figure S8.** **a)**  $^1\text{H}$  projection extracted from the  $^1\text{H}$ - $^7\text{Li}$  HETCOR and **b)**  $^1\text{H}$  projection extracted from the  $^{13}\text{C}$ - $^1\text{H}$  HETCOR presented in Figure 6.